Journal of Materials Chemistry B

Accepted Manuscript

ROYAL SOCIETY OF CHEMISTRY

www.rsc.org/materialsB

Cite this: DOI: 10.1039/c0xx00000x

www.rsc.org/xxxxxx

ARTICLE TYPE

Surface Modified Titania Nanotubes Containing Anti-bacterial Drugs for Controlled Delivery Nanosystems with High Bioactivity

Peilin Huang[‡a], Jingnan Wang[‡b], Shuting Lai [a], Fang Liu [a], Nan Ni[c], Qingyun Cao[d], Wei Liu [a], David Y.B. Deng*[b], Wuyi Zhou*[a]

[a] *Institute of Biomaterial, Department of Applied Chemistry, College of Science, South China Agricultural University, Guangzhou, 510642, China;*
[b] *Research Center of Translational Medicine, the First Affiliated Hospital, Sun Yat-Sen University, Guangzhou 510080, China;*
[c] *College of Materials and Metallurgy, Northeastern University, Shenyang,110004, China.*
[d] *College of Animal Science, South China Agricultural University, Guangzhou, 510642, China*

Corresponding authors, Email: David Y.B. Deng, dengyub@mail.sysu.edu.cn Email: Wuyi Zhou, zhouwuyi@scau.edu.cn

‡ Both authors contributed equally to this work

Surface functionalization of nanomaterials is realized to be vital to fabricate high drug stationary, sustain release, and remarkable *in vivo* biocompatibility and bioavailability drug delivery nanosystems, from which nanomaterials such as titania nanotubes (TNT) can be functionalized and designed as specific drug delivery nanosystems. Here, two kinds of novel drug delivery nanosystems as Enro-NH_2-TNTs and Enro-SH-TNTs were firstly prepared through combining characteristic pH adjustable-recrystal loaded process of enrofloxacin (Enro) and surface silane coupling agent modified titania nanotubes (NH_2-TNTs and SH-TNTs). FTIR analysis exhibited that Enro molecules were interacted with surface grafted groups -NH_2 or -SH through electrostatic effect or hydrogen effect. Enro molecules were recrystallized and loaded into the two type of modified TNTs through such characterizations as X-ray diffusion patterns (XRD), surface area analysis (BET), and transmission electron microscope (TEM). *In vitro* experiments exhibited excellent controlled-release property and further proved that the Enro drugs had been loaded into TiO_2 nanotubes, which were influenced by grafted molecules. *In vitro* cell viability, hemolysis assay and cell apoptosis experiments showed that it could increase biocompatibility and lower cytotoxicity of TNTs nanomaterials to cells by the surface modification. Those modified drug delivery nanosystems owned higher drug bioavailability and longer drug effect through *in vivo* administration to chickens. Surface modification combining with pH adjusted process has large potential in fabricating long-acting drug delivery nanosystems especially with hydrochloride drugs.

Introduction

Titania nanotubes (TNTs) have aroused a lot of interests in fields like drug delivery system,[1] anti-bacterial materials,[2] biomaterials such as tissue and bone regeneration, grow factor carrier, cell behavior regulator and implanted devices,[3] biosensors,[4] etc, for its porous structure, biocompatibility, large surface area, anti-bacterial properties or sterilization, thermal stable and nontoxic properties,[5] etc. What's more, titania nanotubes can enhance effect on blood clotting and hemorrhage stopping,[6] which is in favor of fabricating or designing as series of drug delivery nanosystems. However, pure titania nanotubes, applied as single drug delivery nanosystem with porous structure, could hardly immobilize drug and maintain long term sustain release with less interacted force with drug molecules. Similarly as porous structure such as MCM-41, even the novel drug loaded process reported as pH-adjusted method,[7] it can hardly achieve drug inside stationary and drug controlled release properties since *in vitro* burst release still remained in 24 h with cumulative rate of nearly 60%, which was simply determined by porous matrix structure and hardly performing long term sustain release *in vivo*. Worse still, like other nanoparticles with less binding sites to organs *in vivo*[8] regarding as bioinert nature, single TNTs drug delivery nanosystems could not exert their wide advantages in biomaterials and drug delivery materials, leaving much more to be desired.

Surface functionalization of nanomaterials is realized to be vital, from which TNTs are endowed with advance surfaces and could contribute to a wide range of biomedical applications.[9] Meanwhile, surface functionalizations such as chemical modification,[10] composite coating[11] and etc, can overcome the bioinert of TNTs, increase interaction to tissue[12] and fortify adhesion to cells[13], from which obstacles such as charge or size effect of drug molecules to move through cell membrane could be handled. Meanwhile, selected surface grafted molecules can increase electrostatic and hydrogen bonding effect of nanotubes towards drug molecules. As the result, TNTs can be designed as functionalized drug delivery nanosystems with increasing biocompatibility, bioavailability and long term sustain *in vivo* therapeutic effects.

Here, we firstly report a novel drug delivery nanosystems fabricated through combining surface silane coupling agent modified titania nanotubes and characteristic pH-adjusted drug loading process. Enrofloxacin (Enro), a kind of fluoroquinolone antibiotics drug with broad spectrum,[13] was chosen as the model drug, which remains some side effects such as residual dosages,[14] relatively shorter efficacy term,[15] low bioavailability to be tackled. Pure titania nanotubes and modified titania nanotubes have been respectively studied through fabricating drug delivery nanosystems such as Enro-TNTs, Enro-NH_2-TNTs and Enro-SH-TNTs. Enro molecules were proved to be recrystallized inside nanotubes and interacted with surface modified TNTs through electrostatic effect analyzed by FTIR, XRD and BET. *In vtiro* drug release and cell experiments assess showed that simply inner grafted with -NH_2 or -SH groups, could increase the hydrogen

and electrostatic interacted effects between enrofloxacin and internal nanotubes while outer modified surface providing more binding sites and adhesion of TNTs in improving cell biocompatibility but lowering cytotoxicity. Meanwhile, *in vivo* administration experiment comprehensively revealed modified drug delivery nanosystems could not only prolong drug release term but also ensure drug microbicide effect *in vivo* with longer effective therapy periods, half-time of elimination and extending time of peak in drug therapeutic effect term.

Materials and methods

Reagents and materials

All materials and reagents were used as commercially received. P25 TiO_2 was purchased from Degussa Co., Germany. Thiol silane coupling agent (KH590) and amino silane coupling agent (KH550) were analytical reagent and supported by BYK Additives Co., Germany. Enrofloxacin hydrochloride (Enro·HCl) was supported by Guangzhou Huihua Animal Health Products Co., Ltd, China. Sodium hydroxide was supported by Guangzhou Guanghua Chemical Factory Co., Ltd, China. Hydrochloric acid was supported by Guangzhou Chemical Reagent Factory. Ethyl alcohol was analytical reagent and purchased from Tianjin Fuyu Fine Chemical Co., Ltd, China. Heparin sodium was analytical reagent and purchased from Shanghai Shifeng Biological Technology Co., Ltd, China. Acetonitrile and methanol was HPLC grade reagent and supported by Thermal Fisher Scientific Co., US. Phosphate buffer saline (PBS) solution (0.01 M, pH=7.4) were prepared and used as the solvent for release experiment. All other chemicals were purchased from Sinopharm Chemical Reagent (China) unless otherwise noted.

Synthesis of modified TNTs drug delivery materials

TNTs were synthesized through solvent thermal method,[16] and NH_2-TNTs and SH-TNTs were prepared via a co-condensation method shown in Fig. 1. Briefly, 0.50 g of TNTs was weighed precisely and dispersed in 50 mL xylene with 10 mmol of silicane agent such as KH550 or KH590. The suspension was ultrasound and treated through vacuum processing to vacuum degree of 0.02 MPa for 10 min. The suspension was refluxed for 24 h at 85 □ with stirring rate 200 rpm under N_2 atmosphere. Finally, NH_2-TNTs or SH-TNTs powders were collected by centrifuged with triply washed by xylene and absolute ethanol, and dried in an oven at 40 □ for further use. Modified molecular was bonded to inside and outside surface of TNTs through dehydration condensation process.

Fabrication of Enro-TNTs, Enro-NH_2-TNTs and Enro-SH-TNTs drug delivery nanosystem

Synthesis method of the Enro-TNTs, Enro-NH_2-TNTs and Enro-SH-TNTs drug delivery nanosystem are similar to the typical pH adjustable drug recrystal method.[7] Briefly, 0.100 g of TNTs (or NH_2-TNTs and SH-TNTs) powder was precisely weighed and then 20 mL of deionized water was added into a reactor. After treated with ultrasound for 5 min, 0.200 g of Enro·HCl powder was added and then totally treated by vacuum pumping until a vacuum degree of 0.02 MPa. A certain amount of 2 M NaOH solution was dropwise added to adjust the pH value of the solution to 7.0. The reactor was shaken at room temperature for 48 h and the obtained Enro-TNTs products were collected by an ultrafiltration process. After washed by deionized water triply, the final products were dried in a vacuum oven at room temperature for 24 h. The obtained filtrate was collected and detected by UV-vis spectrophotometer (UV-2550, SHIMADZU) at wavelength of 271 nm to calculate the entrapment efficiency (EE) and loading capacity (LC) of the drugs. Standard curve was drafted as different concentration Enro-PBS solution (c) *vs* UV absorbance (A) at 271 nm, given as equation A = 0.01271c-7.3852, R^2=0.9996, and linear range as 0~0.020 g/L. The equation was shown as below.

$$EE\,\% = \frac{m_{total} - m_{surplus}}{m_{total}} \times 100\,\%$$

$$LC\,\% = \frac{m_{total} - m_{surplus}}{m_{system}} \times 100\,\%$$

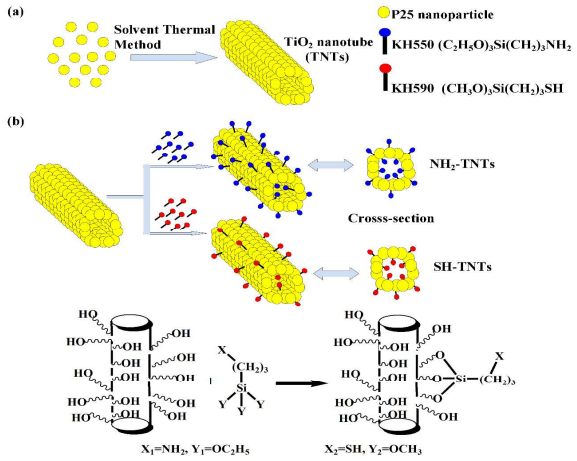

Fig. 1 Mechanism of (a) Synthesis of TNTs through Solvent-Thermal Method and (b) Synthesis of NH_2-TNTs and SH-TNTs through Condensation Method

Characterization

The crystal structure of samples were identified by X-ray diffraction (Cu $K_{\alpha 1}$ irradiation at 40 kV and 20 mA, Bruker D8, Germany, with scanning speed of 4°/min, step width of 0.02° and Cu target with wavelength of 0.15406 nm). FT-IR (360, Nicolet Avatar, SHIMADZU) was used to determine molecular structures of different samples. The porous structure of samples was confirmed by BET (GEMINI VII 2390, Micromeritics). Morphologies and structures of the samples were detected by TEM (G220, Tecnai).

In vitro release property

Briefly, 10 mg of each drug delivery naonsystems' powders was precisely weighed and dispersed into 2 mL of PBS solution (0.01 M, pH=7.4). The dispersion was shifted to a sealed dialysis bag. The dialysis bag was submerged into the PBS solution in 500 mL of conical flask with slow magnetic stirring. The concentrations of drugs released in PBS solution could be monitored by absorbance, which were detected by a UV-vis spectrophotometer (UV-2550, SHIMADZU) with wavelength of 271 nm at given time so as to measure cumulative release rate with standard curve above.

In vitro cell testing

Cytotoxicity and biocompatibility of TNTs, NH_2-TNTs and SH-TNTs were assessed through Cell Counting Kit-8 (CCK-8) and

Hoechst strains experiments with human embryonic kidney (HEK) 293T cells (2500 cells/well) and rat pheochromocytoma PC12 cells (2500 cells/well) incubated. Hemolysis assay was performed using blood from SD rats to evaluate the toxicity of drug delivery materials.

***In vivo* evaluation of drug delivery nanosystems**

24 of yellow-feathered chickens aged 60 days, weighing 1.26±0.29 kg, were purchased from South China Agriculture University Animal Farm, which were divided into female and male equally, and cultivated normally in single cages feeding with fodders without anti-bacterial drugs. Blank blood samples were collected before administration. Administration method was intramuscular injection through drumstick, with dosage of 10 mg/kg (Enro/BW). After administration, each 3 mL of chicken blood samples was collected by injection syringe from wing vessel at measured time. These blood samples were transferred to 5 mL centrifuge tubes wet by few heparin anticoagulant. After centrifuged at 4000 rpm for 10 min, the upper plasma was collected to another 5 mL of centrifuge tube. Then, 0.5 mL of plasma was accurately added to a 5 mL of centrifuged tube and mixed with 1 mL of methanol. The tube was treated by a 10000 rpm centrifuge for 15 min. The upper solution was filtrated and transferred to 2 mL of auto injected sample bottle for analysis by UHPLC assay (WATERS ACQUITY UHPLC, America) with specific instrument condition. Fluorescence detector with excitation wavelength of 278 nm and emission wavelength of 465 nm was chosen. The chromatographic column was Hypersil BDS C18 (4.6 mm×250 mm, 5 μm). Mobile phase was 0.05 M citric acid and 0.01 M ammonium acetate buffer, and mixed with acetonitrile as a constant volume ratio (71:29, v:v). Column temperature was 30 □. Samples were injected with constant volume of 10 μL, flow rate of 1.0 mL/min and limit of quantitation of 0.02 μg/mL. The concentration of enrofloxacin in chicken blood was measured through standard curve, and volume relationship due to the sampling process. The standard curve is established as concentration (C, μg/mL) *vs* peak area (μV·S), $C=3.9205\times10^{-7}A-0.01622$, $R^2 = 0.9998$ and liner range is 0.01~10 μg/mL. The recovery for the Enro in blood from three different concentration (0.05, 0.5 and 5 μg/mL) were measured as 97.12±3.53%, 98.24±2.65% and 99.73±4.82%.

Results and discussion

Designed of drug delivery nanosystems

After solvent thermal synthesization of TNTs, NH_2-TNTs and SH-TNTs were synthesized through solvent condensation method with silane coupling agent KH550 and KH590, respectively. They were used to fabricate drug delivery nanosystems. As the process shown in Fig. 2, the Enro drugs were loaded into TNTs, NH_2-TNTs and SH-TNTs through characteristic pH adjusted recrystallization process. Firstly, Enro·HCl was dissolved in deionized water gently, and Enro·H^+ cations were formed. After vacuum processing, air molecules in the internal of TNTs and modified TNTs were moved out, allowing more Enro·H^+ solution to enter into these nanotubes. After adjusted to pH value of 7.0, which is closed to isoelectric point of Enro, zwitterionic formed Enro molecules were generated, and incorporate to inner or outer surface of modified TNTs through different ionic ends. For NH_2-TNTs, -COO^- anonic ends were chosen to incorporated to -NH_3^+ groups on the surface. For SH-TNTs, -NH^+- cationic ends were selected to combine -SH groups on the surface. Through hydrogen bonding effect and electrostatic attractive effect, Enro drugs were loaded into the modified TNTs. For TNTs, Enro was combined to -OH groups on the surface through weak force. With guidance of inner surface grafted molecules, Enro crystals could grow inside the nanotubes in the next 48 hrs' shaking process. Through the dried process in oven, with groups -NH_2 or -SH interacted with Enro molecules inside nanotubes, the modified drug delivery nanosystems could better immobilize Enro molecules inside nanotubes.

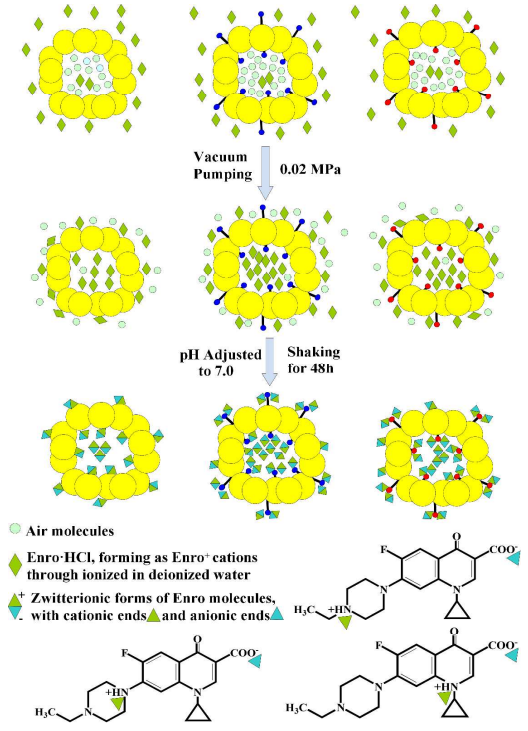

Fig. 2 Fabrication of drug delivery nanosystems

FTIR analysis

Fig. 3(a) shows molecular structure of TNTs and modified TNTs. TNTs mainly owned specific peak at 480 cm^{-1} corresponding to vibration of Ti-O bonds, and absorption band at 3396 cm^{-1} relating to surface vibration of TiO-H bonds or O-H bonds from absorbed water.[17] For NH_2-TNTs, the absorption peak at 3300-3500 cm^{-1} widened for the increase of hydrogen bonding association, which was attributed to the surface grafted -NH_2 groups. Peaks at 2933 cm^{-1} corresponded to stretching vibration of C-H bonds on -CH_2-, which were from the modified KH550 molecules of the surface. Peaks at 1390 cm^{-1} and 1220 cm^{-1} corresponded to vibration of C-N bonds. Peak at 1120 cm^{-1} and 1020 cm^{-1} most probably corresponded to stretching vibration of C-O-Si or Si-O bonds. Peak at 470 cm^{-1} corresponded to bending vibration of Ti-O. SH-TNTs observed in Fig. 3(a) showed stretching vibration absorption peak of C-H bonds at 2927 cm^{-1}. The peak at 2570 cm^{-1} was mostly attributed to deformation vibration of S-H bonds. Peaks at 1259 cm^{-1} was attributed to stretching vibration of S-C bonds. Peaks at 1108 cm^{-1} and 1045 cm^{-1} corresponded to vibration of O-Si or C-O-Si bonds.

The molecular structure exhibited by FTIR analysis in Fig. 3(b), showed drug delivery properties of different nanosystems in detail. For pure Enro shown in Fig. 3, peaks located at 1731 cm^{-1}, 1631 cm^{-1}, 1508 cm^{-1} and 1477 cm^{-1} were attributed to specific vibration of C=O bond of -COOH, bending vibration of -OH, symmetric and anti-symmetric stretching vibration of -COO- groups and $-COO^-$ anionic ends. For Enro-TNTs, Enro-SH-TNTs, and Enro-NH_2-TNTs, specifical peaks of -COO- were increased in turn, which was an evidence that Enro molecules were successfully loaded into TNTs and modified TNTs through vacuum process-pH adjusted method. We found that peak at 1392 cm^{-1} corresponded to deformation vibration of O-H bonds on -COOH groups had lowered through recrystallized process loaded into TNTs from which we could judge that recrystallized Enro was internal salt compared with pure Enro. It was noted that several peaks at 2700~2500 cm^{-1} corresponded to stretching and deformation vibration of O-H bonds from dissociative -COOH groups in Enro-SH-TNTs, which showed that -SH groups had interacted with -NH- groups of Enro molecules, and partly replaced the effect of -COOH with -NH- intramolecularly. While in Enro-TNTs and Enro-NH_2-TNTs, peaks at 2500 cm^{-1} could not be observed for both dissociative -COOH groups decreased. Because in Enro-TNTs, recrystallized Enro was internal salt and -COOH was reacted with -NH-, and in Enro-NH_2-TNTs, partial -COOH interacted with $-NH_2$ on the surface of NH_2-TNTs. Those were evidences that the modified TNTs increased electrostatic attractive effect between Enro and the drug delivery materials.

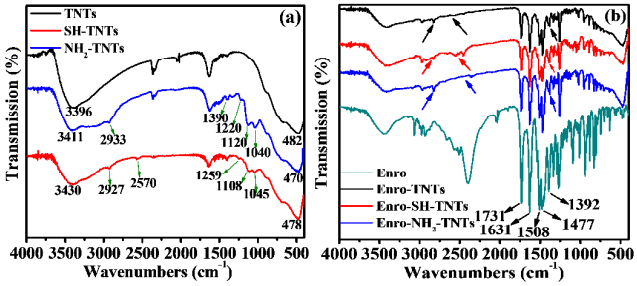

Fig. 3 FTIR of different samples: (a) drug delivery materials, TNTs, NH_2-TNTs and SH-TNTs; (b)Enro, Enro-TNTs, Enro-NH_2-TNTs and Enro-SH-TNTs

XRD

XRD pattern of the samples shown in Fig. 4(a) indicated the crystal structure of P25 nanoparticles, and drug delivery materials. TNTs were formed through solvent thermal treatment of P25 nanoparticles and remained weak anatase crystalline phase with the diffraction peaks at $2\theta_{(101)}$=24.18°, $2\theta_{(103)}$=28.12°, $2\theta_{(200)}$=48.08°. The weak diffraction intensity of TNTs, NH_2-TNTs and SH-TNTs showed similarly weak polycrystalline structure. Crystal structure of Enro, Enro-TNTs, Enro-NH_2-TNTs, Enro-SH-TNTs were exhibited by XRD analysis shown in Fig. 4(b). For recrystallized Enro, diffraction peaks were shown in 2θ=14.68°, 2θ=19.08°, and 2θ=25.60° strongly. Since XRD of TNTs and modified TNTs shown in Fig. 4(a) revealed weak polycrystalline, higher diffraction peaks of Enro-TNTs, Enro-SH-TNTs and Enro-NH_2-TNTs in Fig. 4(b) corresponded to the loaded recrystallized enrofloxacin. Peaks at 2θ=14.68°, 2θ=19.08°, and 2θ=25.60° attributed to drug crystalline phase were increased sequentially, Enro-TNTs, Enro-SH-TNTs and Enro-NH_2-TNTs, from which we are confirmed that the modified TNTs drug delivery nanosystems owned higher drug loading capacities compared to single TNTs drug delivery nanosystem.

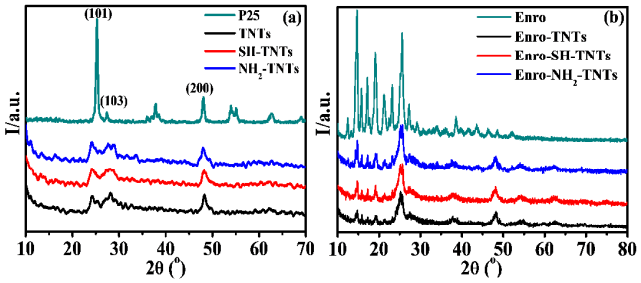

Fig. 4 XRD of different samples: (a) P25 nanoparticles, TNTs, NH_2-TNTs and SH-TNTs; (b)Enro, Enro-TNTs, Enro-NH_2-TNTs and Enro-SH-TNTs

BET analysis

BET experiment using N_2 absorption and desorption to assess the porous structure of TNTs and modified TNTs before and after loading Enro as shown in Fig. 5. It was found that non-specific absorption of TNTs, NH_2-TNTs, SH-TNTs, Enro-TNTs, Enro-NH_2-TNTs and Enro-SH-TNTs, and BJH method was applied to analyze pore distribution. Observed pore size distribution graph in Fig. 5, most pore sizes were equal to inner diameters of nanotubes. The most pore sizes of samples were located at range from 0~50 nm, from which we believed that drug delivery materials and drug delivery nanosystmes were mesoporous matrix structures, which were composed of nanotubes. We realized that after modified process, pore volume of TNTs significantly decreased and most diameters of TNTs as 24.0 nm had slightly decreased to 23.6 nm because the silane coupling agent molecules had successfully grafted to inner surface of TNTs. Moreover, pore volumes of these drug delivery materials were obviously decreased after the Enro loading process. Meanwhile, most inner diameters of TNTs and modified TNTs were decreased after fabricated as drug delivery nanosystems, shown as 23.5 nm of Enro-TNTs, 18.5 nm of Enro-NH_2-TNTs and 21.5 nm of Enro-SH-TNTs, from which we found inner drug layer thickness had increased through surface modification of TNTs. Through combination of surface modification and characteristic pH-adjusted process, inside drug loading properties had improved and Enro molecules were high efficiently loaded inside TNTs and modified TNTs.

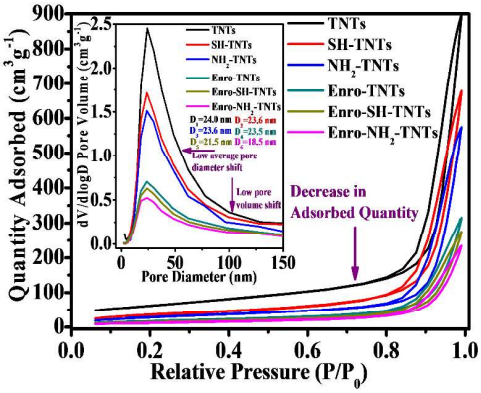

Fig .5 BET analysis of different samples: TNTs, NH_2-TNTs, SH-TNTs, Enro-TNTs, Enro-NH_2-TNTs and Enro-SH-TNTs

TEM

Fig. 6 revealed structure and morphology of different samples. Fig. 6(a-c) showed the TEM images of TNTs, NH_2-TNTs and SH-TNTs samples. The pure TNTs are mainly tubular structure with a width diameter of about 20 nm. However, TNTs modified sample including NH_2-TNTs and SH-TNTs are aggregated due to polar groups such as -NH_2 and -SH on the surface and hydrogen bonding effect, resulting in the accumulation of nanotubes. Drug loaded delivery nanosystems are shown in Fig. 6(d-f). We noted that, after drug loading process, the gaps between TiO_2 nanotubes were full of Enro drugs and the outline of tubular structure became vague in TEM observation. We found that the Enro drugs partly deposited on the TNTs surface by recrystallized drug loading process increased the aggregation of TNTs or modified TNTs carriers, which was attributed to the polar of Enro molecules by forming intermolecular hydrogen bonds and ionic bonds. Surface modified TNTs, with grated molecules and electrostatic effects with Enro molecules, had increased inside nanotubes drug loaded property through characteristic pH adjusted recrystallized method.

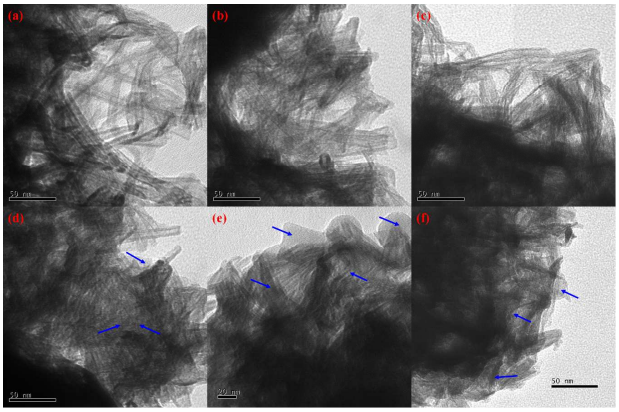

Fig. 6 TEM images of (a) TNTs, (b) NH-TNTs, (c) SH-TNTs, (d) Enro-TNTs, (e) Enro-NH2-TNTs, (f) Enro-SH-TNTs

Loading capacity and entrapment efficiency

In order to analyze improvement of drug loading properties of surface modification and characteristic pH adjusted recrystallized process, we compared drug loading capacity and entrapment efficiency of novel drug delivery nanosystems Enro-TNTs, Enro-NH_2-TNTs and Enro-SH-TNTs and simple drug delivery nanosystmes such as Enro@TNTs, Enro@NH_2-TNTs and Enro@SH-TNTs, which were fabricated through simple absorption force towards drug molecules. Observed in Fig. 7, we found that through characteristic pH adjusted process, drug loading capacity and entrapment efficiency were significantly increased for Enro-NH_2-TNTs, Enro-SH-TNTs and Enro-TNTs compared with simple drug delivery nanosystmes Enro@NH_2-TNTs, Enro@SH-TNTs and Enro@TNTs fabricated through simply absorption force towards drug molecules. Characteristic pH adjusted recrystallized process could force drugs to recrystallize inside drug delivery materials, and increased drug loading efficiency. For Enro-NH_2-TNTs and Enro-SH-TNTs, both modified drug delivery nanosystems owned higher drug loading capacity and entrapment efficiency compared with Enro-TNTs, which were attributed to surface modification of drug delivery materials with amino and thiol groups providing more ionized bonding effect and more hydrogen bonding effect with drug molecules, increasing immobilization of drugs. Combining surface modification and characteristic pH adjusted process, drug loading properties were increased, revealing significantly increased in high efficiency drug loading properties.

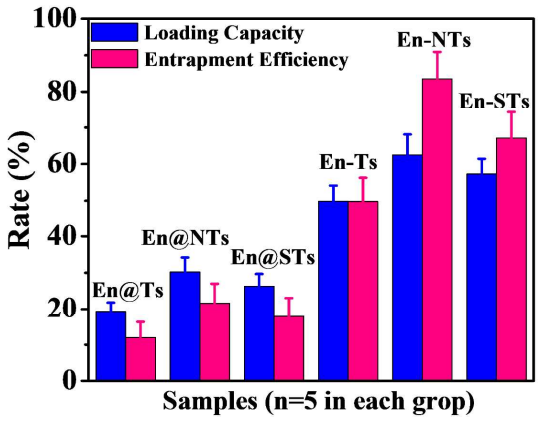

Fig. 7 Drug loading capacity and entrapment efficiency of different samples: Enro@TNTs(Enro@Ts), Enro@NH_2-TNTs(Enro@NTs), and Enro@SH-TNTs(Enro@STs), Enro-TNTs(En-Ts), Enro-NH_2-TNTs(En-NTs) and Enro-SH-TNTs(En-STs); (Enro@TNTs, Enro@NH_2-TNTs and Enro@SH-TNTs were fabricated through mixing 0.1 g of drug delviery materials and 0.2 g of Enro·HCl in 20 mL PBS (0.01 M pH=7.0) suspensions with 48 hs' shaking in reactor at room temperature)

***In vitro* release of drug delivery nanosystmes**

Only quantitively high drug loading properties were not enough since we are pursuing long term sustain release, which is determined by high inside-nanotubes drug loading properties and interaction effect of surface grafted molecules. *In vitro* release experiments were performed for drug delivery nanosystems such as Enro@TNTs, Enro@NH_2-TNTs, Enro@SH-TNTs, Enro-TNTs, Enro-NH_2-TNTs and Enro-SH-TNTs. Observed in Fig. 8(a), we observed obvious burst release of Enro@TNTs, Enro@NH_2-TNTs, Enro@SH-TNTs, since cumulative release rates were 41.15±3.10%, 21.53±3.40% and 20.78±3.72% at 0.5 h. In addition, release quantities at 12 h were 80.75±6.82%, 62.12±3.98% and 57.75±4.26% for Enro@TNTs et al, in turn, which showed high cumulative release rate and drugs were mostly concentrated on the surface of drug delivery materials. Only absorption process could hardly fabricate drug delivery nanosystems with high inside-nanotubes' drug loaded efficiency and long release term. Drug delivery nanosystems such as Enro-TNTs, Enro-NH_2-TNTs and Enro-SH-TNTs had increased in long term release properties which were observed in Fig. 8(b). Initial release quantities at 0.5 h were 19.30±0.56%, 9.48±0.77% and 8.13±0.45% for Enro-TNTs, Enro-NH_2-TNTs and Enro-SH-TNTs in turn, respectively, revealing low burst release of these nanosystems. What's more, low release quantities at 24 h were observed such as 45.43±2.83% for Enro-TNTs, 36.39±2.64% for Enro-NH_2-TNTs, and 29.46±2.12% for Enro-SH-TNTs, revealing increased release terms contributed by inside drug loaded properties through characteristic pH adjusted process.

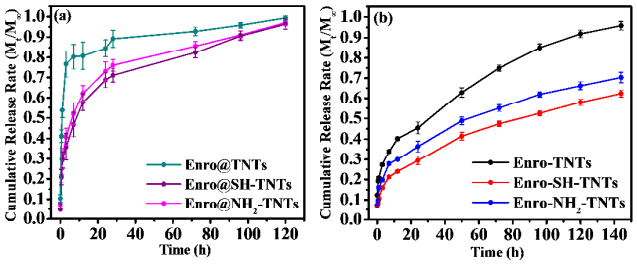

Fig. 8 *In vitro* drug release of different nanosystems

In order to further analyze drug loading properties of Enro-TNTs, Enro-NH_2-TNTs and Enro-SH-TNTs, we divided their release curves in surface controlled process and matrix controlled process shown in Fig.9. The inflection points could be seen obviously in release curves of the three drug delivery nanosystems. Surface controlled release of the drug delivery nanosystems was located before inflection points which reflected surface drug release circumstances and surface drug proportions. The lower drug concentrated on the surface of the modified drug delivery nanosystems is observed at 7 h, such as 21.32±1.09% for Enro-SH-TNTs and 27.85±0.89% for Enro-NH_2-TNTs compared with Enro-TNTs as 40.19±1.29% observed at 12 h, which showed decrease of burst release and increase of inside-nanotubes drug loading efficiency through surface grafted amino groups and thiol groups. Simply vacuum processing and pH adjusted method could obviously increase crystallizable drug loading capacity, but can hardly stabilize drugs inside the delivery nanosystem without any bonding effect to drug molecules. After dried in the oven, drug could reach the surface along with the volatilization of the solvent, decreasing in sustainable release properties. Inner surface modified had lowered Enro in the surface, and increased drug inside stationary properties of modified nanosystems.

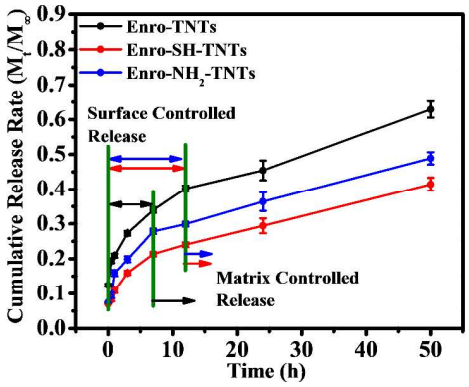

Fig. 9 Division of *in vitro* release curves of Enro-TNTs, Enro-NH_2-TNTs and Enro-SH-TNTs into two controlled release stages

Three pharmacokinetic models (Zero-order, First-order and Higuchi) were applied to study suface controlled part and matrix controlled part of release curves of Enro-TNTs, Enro-NH_2-TNTs and Enro-SH-TNTs as shown in Fig. S1 (ESI†), and the related kinetic parameters were also analyzed in Table S1 (ESI†), so as to find out release mechanism of these drug delivery nanosystems. According to the fitting results, Zero-order and First-order models were not proper to describe the release mechanism of these delivery nanosystems, which were fabricated through pH adjusted process with high inside nanotubes' drug loading efficiency. Both parts of release curve of Enro-TNTs were fitted appropriately by Higuchi equations, from which we consider that the release mechanism of drug from pure TNTs depended simply on the tubular porous matrix in the whole measured time and was in line with Fick's law. Observed correlation indexes in Table S1, the release mechanisms of both modified drug delivery nanosystems deviated Higuchi equations, which were influenced by steric hindrance effect and electrostatic effect of surface grafted molecules. Release mechanisms of Enro were not only dependent on porous structure, but also affected by surface molecules. The amphoteric Enro molecules with -NH- and -COOH groups together can form cations or anions up to different pH values.[18] Controlled release of modified drug delivery nanosystems in PBS solution, on account of higher pH value than isoelectric point of Enro (pH=7.02), much Enro anions (E^-) with -COO^- groups anions were forming in drug delivery nanosystems. Surface modified nanosystems, with electronegative groups such as -NH_2 and -SH, presented electronegative property on the surface of TNTs so as to repulsively interacts with E^- and slowed down diffusion of E^-, from which charge repulsion effect should overcome before release. After surface controlled release process, release behaviors of these two drug delivery nanosystems were dominated by matrix controlled process. Release curves of these two drug delivery nanosystems were fitted properly by Higuchi equations shown in Fig. S1 and Table S1, in which the release mechanism mostly depended on tubular porous framework for solute and diffused internal drugs, and the release mechanism was described by Higuchi model properly. But both drugs release of the modified nanosystems had been slowed down in matrix controlled process compared with Enro-TNTs, since inner grafted groups -NH_2 and -SH increased electrostatic effect or hydrogen bonding effects with Enro molecules. Outer and inner surface modified molecules had hydrogen binding and electrostatic attractive effect with enrofloxacin molecules in drug delivery nanosystems, which slowed drug release rate and increased drug inside stationary for drug delivery nanosystems.

In summary, through qualitatively and quantitatively analysis of different drug delivery nanosystems, we found that Enro drugs inside TiO_2 nanotubes' loaded properties were increased in both modified drug delivery nanosystems, through hydrogen bonding and electrostatic affect between Enro molecules and drug delivery materials.

In vitro cell testing

Biocompatibility or bioactivity of drug delivery nanosystems was mostly determined by drug delivery materials. In order to assess biocompatibility of the drug delivery nanosystems, TNTs, NH_2-TNTs and SH-TNTs were conducted for *in vitro* cell testing such as cell viability, hemolysis assay and cell apoptosis with concrete steps shown in ESI†. Cell Counting Kit-8 (CCK-8) was conducted to assess the cytotoxicity and surface biocompatibility of TNTs, NH_2-TNTs and SH-TNTs, respectively, with human embryonic kidney (HEK) 293T cells (2500 cells/well) in Fig. 10(a) and rat pheochromocytoma PC12 cells (2500 cells/well) in Fig. 10(b) incubated quantitively. TNTs did not show any significant effect on cell viability, establishing the low cytotoxicity of these delivery nanomaterials with concentration

ranged from 15.6-250 mg/L. However, the increased concentration of TNTs such as 500-1000 mg/L showed obviously increased cytotoxicity to both cells. NH_2-TNTs and SH-TNTs maintained significant ($P<0.05$) higher cell viability while concentration increased to 500 mg/L and 1000 mg/L, which showed significantly higher cell viability compared with pure TNTs. To investigate the blood cell biocompatibility and toxicity of the TNTs and modified TNTs, different concentrations of materials PBS suspension were incubated with blood samples from SD rats. The hemolysis rate results in Fig. 11 showed that almost no hemolysis of red blood cells (RBCs) was detected with the concentrations of samples ranging from 31.25 μg/mL to 500 μg/mL, and about 12% hemolytic activity was observed at the high concentration of 1000 mg/L. Most of all, SH-TNTs and NH_2-TNTs showed lower hemolysis rate at concentration of 1000 mg/L compared with TNTs, from which we believe that modification of TNTs could reduce the toxicity and increase biocompatibility to blood cells. Hoechst strain experiment was conducted and seen in Fig. 12 with PC12 cells and Fig. S2 with 293T cells. Results visually showed these three materials had almost no cytotoxicity effect even in a high concentration of 2000 mg/L, since few deformed cell nucleus were observed. The above results indicated the low cytotoxicity and increasing biocompatibility of surface modified of TNTs, such as NH_2-TNTs and SH-TNTs.

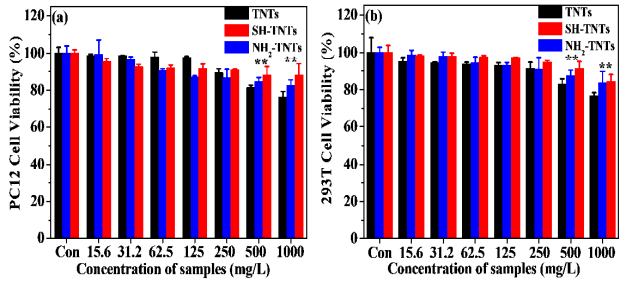

Fig. 10 *In vitro* cell cytotoxicity experiment using (a) rat pheochromocytoma PC12 cells (2500 cells/well), (b) human embryonic kidney (HEK) 293T cells (2500 cells/well), with TNTs, NH_2-TNTs and SH-TNTs PBS suspensions from 15.6 to 1000 (mg/L); (**P<0.05, significant differences compared with TNTs)

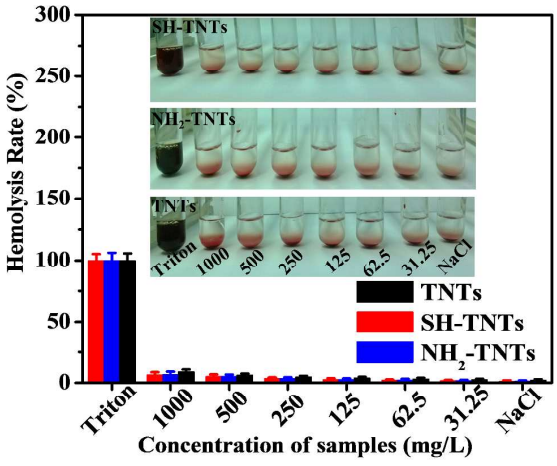

Fig. 11 Hemolysis assay assessments of TNTs, NH_2-TNTs and SH-TNTs PBS suspensions with concentration from 31.25 to 1000 (mg/L)

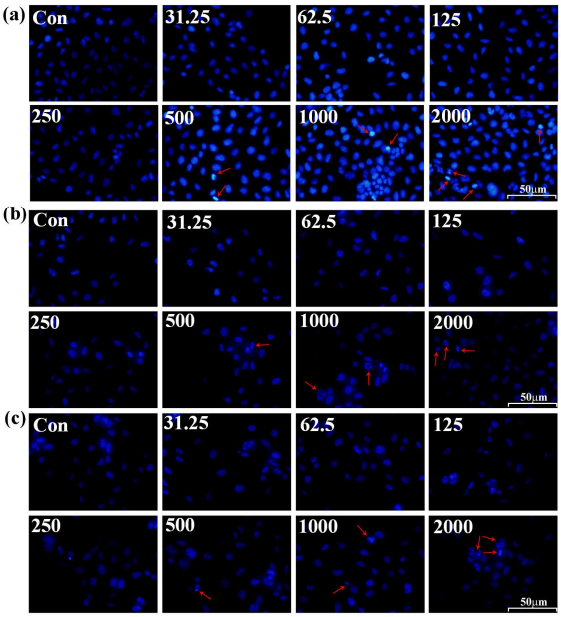

Fig. 12 Immunofluorescence microscopy analysis of apoptosis in PC12 cells induced by different samples (a) TNTs, (b) NH_2-TNTs and (c) SH-TNTs at different concentrations(ranging from 31.25 to 2000 μg/mL) for 72 h. Red arrows indicated apoptosis cells. These drug delivery materials did not have any significant effect on the nucleuses (blue) stained with hoechst33342. Scale bar: 100 μm.

In vivo assessing of drug delivery nanosystmes

In vivo release profiles were simply observed in Fig. 13. Single intramuscular administration of Enro reached peak concentration 2.76±0.15 μg/mL at 1 h and maintained at a proper level of Enro in blood as above 0.2 μg/mL at 24 h. The intramuscular administration of drug delivery nanosystems including Enro-TNTs, Enro-NH_2-TNTs and Enro-SH-TNTs owned reasonable high peak concentration and longer drug eliminated time as 120 h shown in Fig. 13. Minimum therapeutic blood concentration was 0.1 μg/mL for poultry. More than 0.1 μg/mL of Enro could be kept for 72 h by administration of Enro-NH_2-TNTs and Enro-SH-TNTs, which was very conducive for maintaining effective drug concentrations *in vivo*, and increasing long lasting microbicide effect as well.

Pharmacokinetics of pure Enro, Enro-TNTs, Enro-NH_2-TNTs and Enro-SH-TNTs released *in vivo* were studied and parameters could gain through fitting different models, which were shown in ESI†. *In vivo* drug pharmacokinetic parameters were calculated through fitting through proper models with parameters shown in Table S2 (ESI†). Both modified drug delivery nanosystems owned longer term effect of enrofloxacin, such as significantly larger ($P<0.05$) MRT value, $T_{1/2\beta}$ value and less Cl-F values compared with Enro-TNTs and single Enro solution, which revealed longer drug effect terms. However, in addition to long retention time *in vivo*, microbicide effect of enrofloxacin depends on peak concentrations and higher AUC values. Single drug delivery nanosystems such as Enro-TNTs, with less binding sites to enrofloxacin, could merely control drug release by Fick diffusion and promptly reached peak concentration 2.13±0.09 μg/mL at 2 h. Both modified TNTs drug delivery nanosystems had appropriate peak concentrations as 2.63±0.14 μg/mL for

Enro-SH-TNTs achieved at 4.0±0.0 h and 1.98±0.01 μg/mL for Enro-NH_2-TNTs achieved at 3.9±0.1 h, through stationary effect of enrofloxacin by inner grafted groups, increasing drug delivery effect and prolong time of peak *in vivo* to assure long term microbicide effect. Furthermore, Enro-SH-TNTs and Enro-NH_2-TNTs both owned notable larger $AUC_{0\text{-}24h}$ and $AUC_{0\text{-}\infty}$ values compared with Enro-TNTs and Enro solution, highly increased in bioavailability in 24 h and total drug effect periods by the stationary effect of inner surface grafted molecules towards Enro molecules, which were also attributed to the enhancement of inside TiO_2 nanotubes' drug loading properties through characteristic pH adjusted drug loading process. For Enro-TNTs and pure Enro, $AUC_{0\text{-}24h}$ values were almost equal to $AUC_{0\text{-}\infty}$ values, which shown that they mostly performed in 24 h with short drug effect terms. A long lasting drug effect and higher biocompatibility to organ were provided by modified TNTs drug delivery nanosystems since they could perform drug effect even from 24 h to 120 h with obvious larger $AUC_{0\text{-}\infty}$ values compared with $AUC_{0\text{-}24h}$ values. Electronegative groups such as -SH and -NH_2 could increase interaction effects of drug delivery nanosystems and cells with electropositive surface through charge attraction. The Enro molecules might deliver through "bridges" between outer surface grafted groups of modified TNTs and cells, which could increase the transfer of Enro drugs through improvement of drug delivery effects. And long term effects were determined by inner surface modified groups to ensure longer drug effect terms and time of peaks. Drugs *in vivo* release of these two modified drug delivery nanosystems were controllable since enrofloxacin would completely eliminate from blood before 120 h. These results revealed that the modified TNTs drug delivery nanosystems had improved drug relative bioavailability, biocompatibility and therapy effect terms for poultry.

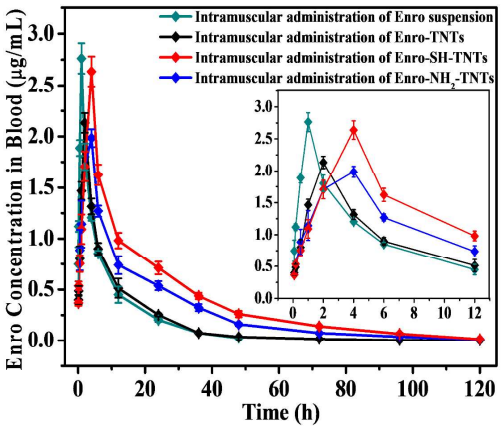

Fig. 13 *In vivo* assess of pharmacokinetics of pure drug agent and drug delivery nanosystems

Conclusions

Novel drug delivery nanosystems, such as Enro-NH_2-TNTs and Enro-SH-TNTs, were successfully synthesized through vacuum processing and pH adjusted method using NH_2-TNTs and SH-TNTs as drug delivery materials. Through XRD, IR, BET and TEM analysis, Enro molecules were found to interact with modified TNTs through ionic bonds or hydrogen bonds. Modified TNTs drug delivery nanosystems with inner surface grafted groups -NH_2 and -SH could stabilize Enro inside nanotubes possessed higher sustained drug release term and less brust release by interacted with Enro molecules through ionic and hydrogen bonding effects compared with single Enro-TNT drug delivery nanosystem. Modified TNTs drug delivery materials showed the increasing biocompatibility and maintained low cytotoxicity of modified TNTs with -NH_2 and -SH groups grafted outer surface, compared with pure TNTs. The *in vivo* administration experiments towards chickens comprehensively showed increase in bioavailability, biocompatibility and longer drug effect of enrofloxacin by agenting as the modified TNTs drug delivery nanosystems. They have large potentials in fabricating as drug delivery nanosystems for hydrochloride drugs.

Acknowledgements

The work was supported by the National Natural Science Foundation (P. R. China, No. 31101854 and 21207041), the Key Academic Program of 211 Project of South China Agricultural University (2009B010100001) and Excellent Scholars with Studying−abroad experiences Funded by the China Ministry of Personnel (2012-2013), and Guangdong Province Production - Study Combination Research Project (No.2012B091100457).

Notes and references

1 (a)C. Moseke, F. Hage, E. Vorndran and U. Gbureck, *Appl. Surf. Sci.*, 2012, **258**, 5399-5404; (b)M. S. Aw and D. Losic, *Int J Pharm*, 2013, **443**, 154-162; (c)P. Rajesh, N. Mohan, Y. Yokogawa and H. Varma, *Mater Sci & Eng C-Mater*, 2013, **33**, 2899-2904; (d)N. K. Shrestha, J. M. Macak, F. Schmidt-Stein, R. Hahn, C. T. Mierke, B. Fabry and P. Schmuki, *Angew Chem Int Edit*, 2009, **48**, 969-972; (e)E. Gultepe, D. Nagesha, S. Sridhar and M. Amiji, *Adv Drug Deliver Rev*, 2010, **62**, 305-315.

2 (a)A. Roguska, M. Pisarek, M. Andrzejczuk and M. Lewandowska, *Thin. Solid. Films.*, 2014, **553**, 173-178; (b)H. R. Li, Q. Cui, B. Feng, J. X. Wang, X. Lu and J. Weng, *Appl. Surf. Sci.*, 2013, **284**, 179-183.

3 (a)Y. Hu, K. Y. Cai, Z. Luo, D. W. Xu, D. C. Xie, Y. R. Huang, W. H. Yang and P. Liu, *Acta. Biomater.*, 2012, **8**, 439-448; (b)Y. H. Lee, G. Bhattarai, I. S. Park, G. R. Kim, G. E. Kim, M. H. Lee and H. K. Yi, *Biomaterials*, 2013, **34**, 10199-10208; (c)L.Zhao, S. Mei, P. K. Chu, Y. Zhang and Z. Wu, *Biomaterials*, 2010, **31**, 5072-5082; (d)L. Z. Zhao, H. R. Wang, K. F. Huo, X. M. Zhang, W. Wang, Y. M. Zhang, Z. F. Wu and P. K. Chu, *Biomaterials*, 2013, **34**, 19-29; (e)A. W. Tan, B. Pingguan-Murphy, R. Ahmad and S. A. Akbar, *Ceram. Int.*, 2012, **38**, 4421-4435; (f)L. Z. Zhao, L. Liu, Z. F. Wu, Y. M. Zhang and P. K. Chu, *Biomaterials*, 2012, **33**, 2629-2641.

4 A. K. M. Kafi, G. Wu and A. Chen, *Biosensors and Bioelectronics*, 2008, **24**, 566-571.

5 (a)S. J. Cho, H. J. Kim, J. H. Lee, H. W. Choi, H. G. Kim, H. M. Chung and J. T. Do, *Mater. Lett.*, 2010, **64**, 1664-1667; (b)N. Caliskan, C. Bayram, E. Erdal, Z. Karahaliloglu and E. B. Denkbas, *Mater. Sci. & Engin. C-Mater.*, 2014, **35**, 100-105; (c)L. Z. Zhao, S. L. Mei, W. Wang, P. K. Chu, Z. F. Wu and Y. M. Zhang, *Biomaterials*, 2010, **31**, 2055-2063; (e)K. C. Popat, M. Eltgroth, T. J. LaTempa, C. A. Grimes and T. A. Desai, *Biomaterials*, 2007, **28**, 4880-4888; (f)K. S. Brammer,

C. J. Frandsen and S. Jin, *Trends Biotechnol*, 2012, **30**, 315-322; (g)S. Wadhwa, C. Rea, P. O'Hare, A. Mathur, S. S. Roy, P. Dunlop, J. A. Byrne, G. Burke, B. Meenan and J. A. McLaughlin, *J Hazard Mater*, 2011, **191**, 56-61; (h)C. Mirjolet, A. L. Papa, G. Crehange, O. Raguin, C. Seignez, C. Paul, G. Truc, P. Maingon and N. Millot, *Radiother Oncol*, 2013, **108**, 136-142.

6 S. C. Roy, M. Paulose and C. A. Grimes, *Biomaterials*, 2007, **28**, 4667-4672.

7 F. Liu, H. Zhang, Q. Cao, X. Xiang, L. Wang, T. He, W. Liu, Y. Fang, D. Y. B. Deng and W. Zhou, *RSC. Advances.*, 2014, **4**, 8918-8921.

8 D. Tarn, C. E. Ashley, M. Xue, E. C. Carnes, J. I. Zink and C. J. Brinker, *Accounts Chem. Res.*, 2013, **46**, 792-801.

9 K. Vasilev, Z. Poh, K. Kant, J. Chan, A. Michelmore and D. Losic, *Biomaterials*, 2010, **31**, 532-540.

10 S. Ban, Y. Iwaya, H. Kono and H. Sato, *Dent Mater*, 2006, **22**, 1115-1120.

11 S. Rammelt, T. Illert, S. Bierbaum, D. Scharnweber, H. Zwipp and W. Schneiders, *Biomaterials*, 2006, **27**, 5561-5571.

12 W. Tan, H. Zhao, N. Ren, J. Li, G. Li, G. Wang, F. Wei, R. I. Boughton and H. Liu, *Ultrason Sonochem*, 2013, **20**, 216-221.

13 (a)W. Yan, S. Hu and C. Y. Jing, *J. Colloid. Interf. Sci.*, 2012, **372**, 141-147; (b)R. Krebber, F. J. Hoffend and F. Ruttmann, *Anal. Chim. Acta.*, 2009, **637**, 208-213; (c)G. H. Wu, Y. Meng, X. H. Zhu and C. Huang, *Anal Biochem*, 2006, **358**, 25-30.

14 (a)Y. K. Kim and H. Kim, *J. Ind. Eng. Chem.*, 2009, **15**, 229-232; (b)S. Kim, J. Ko and H. B. Lim, *Anal. Chim. Acta.*, 2013, **771**, 37-41; (c)A. Rico, M. R. Dimitrov, R. Van Wijngaarden, K. Satapornvanit, H. Smidt and P. J. Van den Brink, *Aquat. Toxicol.*, 2014, **147**, 92-104.

15 (a)S. Xie, L. Zhu, Z. Dong, X. Wang, Y. Wang, X. Li and W. Zhou, *Colloid. Surface. B*, 2011, **83**, 382-387; (b)J. J. de Lucas, J. L. Navarro, S. Rubio, P. E. Vignolo, V. C. Asis, F. Gonzalez and C. Rodriguez, *Vet. J.*, 2008, **175**, 136-138.

16 S. T. Lai, W. Zhang, F. Liu, C. Wu, D. P. Zeng, Y. X. Sun, Y. H. Xu, Y. P. Fang and W. Y. Zhou, *J. Nanosci. Nanotechno.*, 2013, **13**, 91-97.

17 N. F. Fahim, M. F. Morks and T. Sekino, *Electrochim. Acta.*, 2009, **54**, 3255-3269.

18 W. Yan, J. F. Zhang and C. Y. Jing, *J. Colloid. Interf. Sci.*, 2013, **390**, 196-203.

Cite this: DOI: 10.1039/c0xx00000x

www.rsc.org/xxxxxx

ARTICLE TYPE

Surface Modified Titania Nanotubes Containing Anti-bacterial Drugs for Controlled Delivery Nanosystems

Peilin Huang[‡a], Jingnan Wang[‡b], Shuting Lai [a], Fang Liu [a], Nan Ni[c], Qingyun Cao[d], Wei Liu [a], David Y.B. Deng*[b], Wuyi Zhou*[a]

[a] *Institute of Biomaterial, Department of Applied Chemistry, College of Science, South China Agricultural University, Guangzhou, 510642, China;*
[b] *Research Center of Translational Medicine, the First Affiliated Hospital, Sun Yat-Sen University, Guangzhou 510080, China;*
[c] *College of Materials and Metallurgy, Northeastern University, Shenyang,110004, China.*

[d] *College of Animal Science, South China Agricultural University, Guangzhou, 510642, China*

Corresponding authors, Email: David Y.B. Deng, dengyub@mail.sysu.edu.cn Email: Wuyi Zhou, zhouwuyi@scau.edu.cn

‡ Both authors contributed equally to this work

Graphical abstract

Drug delivery nanosystems designed as Enro-NH_2-TNTs and Enro-SH-TNTs with high bioactivity and excellent *in vitro* and *in vivo* controlled release.